Fluorine–Induced Enhancement of the Oxidation Stability and Deep–Blue Optical Activity in Conductive Polyfluorene Derivatives

ARTICLE *in* THE JOURNAL OF PHYSICAL CHEMISTRY C · NOVEMBER 2013

Impact Factor: 4.77 · DOI: 10.1021/jp409996m

5 AUTHORS, INCLUDING:

Arrigo Calzolari
Italian National Research Council
108 PUBLICATIONS **1,904** CITATIONS
SEE PROFILE

Alice Ruini
Università degli Studi di Modena e Reggio Emilia
79 PUBLICATIONS **1,688** CITATIONS
SEE PROFILE

Tersilla Virgili
Italian National Research Council
78 PUBLICATIONS **1,451** CITATIONS
SEE PROFILE

Mariacecilia Pasini
Italian National Research Council
67 PUBLICATIONS **879** CITATIONS
SEE PROFILE

THE JOURNAL OF PHYSICAL CHEMISTRY C

Article

pubs.acs.org/JPCC

Fluorine-Induced Enhancement of the Oxidation Stability and Deep-Blue Optical Activity in Conductive Polyfluorene Derivatives

Arrigo Calzolari,*[,†,‡] Barbara Vercelli,[§] Alice Ruini,[†,∥] Tersilla Virgili,[⊥] and Mariacecilia Pasini[#]

[†]CNR-NANO Istituto Nanoscienze, Centro S3, I-41125 Modena, Italy

[‡]Physics Department, University of North Texas, Denton Texas 76203 United States

[§]Istituto CNR per l'Energetica e le Interfasi, I-20125 Milano, Italy

[∥]Dipartimento di Fisica, Informatica e Matematica, Università di Modena e Reggio Emilia, I-41125 Modena, Italy

[⊥]Istituto CNR di Fotonica e Nanotecnologie, 20132 Milano, Italy

[#]Istituto CNR per lo Studio delle Macromolecole, 21133 Milano Italy

Supporting Information

ABSTRACT: We present a joint experimental/theoretical study on the effects of fluorination on structural, electronic, and optical properties of poly[(9,9-di-*n*-octylfluoren-2,7-diyl)-alt-tetrafluoro-*p*-phenylene] (PFTFP), a polyfluorene (PFO)-derived conjugated polymer. The combination of optical (UV−vis) and electrochemical (cyclic voltammetry) techniques with atomistic simulations demonstrates an improved oxidative stability of the fluorinated compound with respect to standard PFO. The resulting excellent luminescence efficiency along with the preservation of the good charge mobility, characteristic of the pristine PFO, make PFTFP a superior material for optoelectronic applications in the deep-blue. The comparison with auxiliary model systems provides a microscopic identification of the peculiar effects of fluorine on the structural and electronic properties of the polymer.

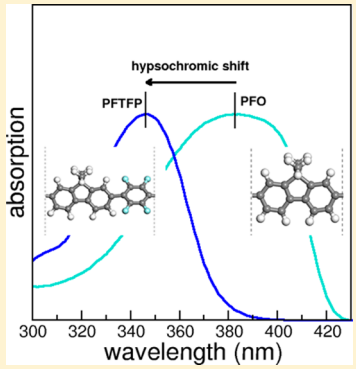

1. INTRODUCTION

Fluorinated conjugated compounds, typically molecules and oligomers, are attracting an increasing interest as functional organic material for optoelectronic devices and liquid crystals.[1] The specific features of fluorinated compounds are related to the halogen atom properties, such as the high electronegativity, which is responsible for the high bond energy and the strong polarization of the C−F bond.[2] One of the effects due to the introduction of electron-withdrawing substituents, such as fluorine atoms, is the energy lowering of the frontier orbitals, for example, the highest occupied (lowest unoccupied) molecular orbital HOMO (LUMO). The down-shift of the HOMO implies an enhancement of the oxidative stability and thus an improvement of the stability in air of the polyconjugated materials, while the lowering of the LUMO may facilitate the electron injection into anodic contacts. The charge polarization and the resistance against oxidative degradation[3] simplify the device fabrication and operation conditions[4] and represent a promising strategy to enhance the performance of the material as emitting layer in OLEDs,[3,5] high-dielectric-constant organic gate in field-effect transistors (OFETs),[6] and organic photovoltaic (OPV) devices.[7]

Despite the large number of reports on the fluorine-induced oxidative stabilization,[3,8] several questions remain still open: for example, the effect of fluorination on the energy-gap is not completely clear. Indeed, since the down-shift of the HOMO/LUMO states is not rigid, both narrowing and widening of optical gap (i.e., red- and blue-shifts in the optical spectra) have been observed depending on the specific system: considerable red-shift was in fact reported following fluorination of oligoacenes,[9] porphyrins,[10] up to finite graphene nanoribbons,[11] while blue-shifted spectra were detected in the case oligothiophenes[12] and PPV-based oligomers and polymers.[13] The microscopic origin of these different behaviors upon fluorination is not yet completely understood and is alternatively attributed either to structural modifications or to mere electrostatic effects.

Finally, while fluorinated molecules and short oligomers have been successfully exploited for the realization of organic semiconductors, fluorination of soluble polyconjugated polymers is still a major challenge that has not been investigated in detail. The first attempts are appearing in these days for the synthesis of highly performing n-type polymers for OFET[14] and photovoltaic[15] applications. Although the development of brand-new polycondensation reactions has recently emerged,[16,17] the full achievement of perfluorinated polyconjugated materials as efficient deep-blue emitter is still only an expectation.

Received: October 8, 2013
Revised: November 18, 2013
Published: November 28, 2013

Scheme 1. Molecular Structure of PFO, PFTFP, and PFP

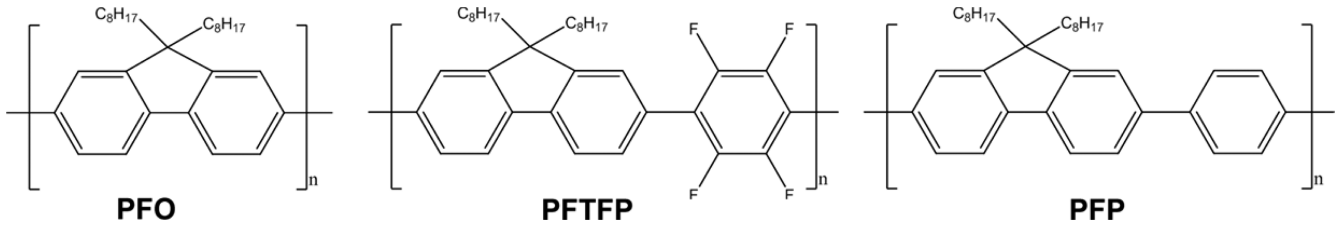

The most studied and applied materials as organic blue emitters are polyfluorene (PFO)-based polymers.[18] PFO (Scheme 1) is a π-conjugated wide-bandgap material with a carbon-only backbone, which exhibits high charge (hole) mobility and strong electroluminescence. Nonetheless, PFO-based OLEDs[19] are known to suffer from poor stability (exhibited by efficiency loss) and from the appearance of a green emission after a short operation time due to keto defects caused by photo-oxidative degradation and thermal instability.[20] Even though the green polyfluorene emission can be quenched by changing the device configuration and incorporating a suitable hole-transporting layer[21] and keto effects can be reduced by using completely 9,9-difunctionalized fluorene monomers, the purity of the difunctional monomers is crucial. Fluorination could be an attractive answer to this drawback:[18] the introduction of fluorine in PFO-derived systems as an electron-withdrawing substituent is expected to give a pure deep-blue material by increasing the energy bandgap and to facilitate the electron injection through a balanced charge injection.[3] Unfortunately, the fluorination of conjugated polymers often[13,22] causes massive structural distortions, which damage the electronic conjugation along the chain and strongly reduce the carrier mobility of the material. This is highly detrimental for the final OLED efficiency.

Recently a PFO-based copolymer with a fluorinated phenylene unit, poly[(9,9-di-*n*-octylfluoren-2,7-diyl)-alt-tetrafluoro-*p*-phenylene] (PFTFP)[23] (see Scheme 1), has been synthesized using an optimized Suzuki cross coupling. This polymer presents a deep-blue photoluminescence (PL) emission at 405 nm with a photoluminescence quantum yield (PLQY) of ≈68%, surprisingly retained also in the solid state. The use of this polymer has also been successfully tested in OLED devices reaching very good results (5.03% external quantum efficiency),[23] giving the first unambiguous proof of fluorination efficacy in achieving pure deep-blue electroluminescence in a highly efficient and stable OLED. Despite this brilliant success, the main characteristics of PFTFP and the effects of fluorination remain elusive.

In this paper, we present a combined experimental–theoretical investigation of fluorination effects on the optical and the electrochemical properties of PFTFP polymer. By using vibrational and optical spectroscopies, along with electrochemical techniques and atomistic simulations, we fully characterize the main intrinsic electronic and optical properties of this new compound. Furthermore, through a comparison with the plain PFO and with the hydrogenated analogous poly[(9,9-dioctylfluorene-2,7-dyil)-alt-*p*-phenylene] (PFP), we investigate the microscopic effects of fluorine substitution on both structural and electronic properties of PFTFP. Our results indicate that the fluorination-effect in PFTFP is mainly ascribed to the electron-withdrawing nature of the four fluorine atoms in the phenylene moiety.

2. METHOD

2.1. Experiments. *Chemicals and Reagents.* Acetonitrile was reagent grade (Uvasol, Merck) with a water content <0.01%. The supporting electrolyte tetrabutylammonium perchlorate (Bu_4NClO_4) and all other chemicals used for characterizations were reagent grade and used as received. Poly[(9,9-di-*n*-dioctylfluoren-2,7-diyl)-(2,3,5,6-tetra-fluoro-1,4-phenylene)] and poly[(9,9-di-*n*-dioctylfluoren-2,7-diyl)-(1,4-phenylene)] were prepared according to the literature.[23] PFO was purchased from American Dye Source.

Apparatus and Procedure: Electrochemistry and Spectroscopy. Experiments were performed at room temperature under nitrogen in three electrode cells using 0.1 M Bu_4NClO_4 as supporting electrolyte. The counter electrode was platinum; reference electrode was a silver/0.1 M silver perchlorate in acetonitrile (0.34 V vs SCE). The voltammetric apparatus (AMEL, Italy) included a 551 potentiostat modulated by a 568 programmable function generator and coupled to a 731 digital integrator. The working electrode for cyclic voltammetry was a carbon-glass working electrode (0.2 cm^{-2}). Optical measurements were performed by a Perkin-Elmer Lambda 600 spectrometer.

2.2. Theory. *Structural and Electronic Properties.* Calculations were performed within the Density Functional Theory (DFT) framework, with planewave basis set and pseudopotentials, as implemented in the Quantum-ESPRESSO package.[24] We adopted hybrid exchange correlation functional (PBE0), which allows for a proper evaluation of the energy gap and energy level alignment. Ionic potentials are described by ab initio norm-conserving pseudopotentials and single-particle wave functions are expanded in a plane-waves basis with an energy cutoff of 60 Ry. A 5 k-point grid is used for summations over the 1D Brillouin zone. Infinite polymers are simulated using a periodically repeated supercell with dimension 13.02 × 25.00 × 25.00 $Å^3$, which ensures a sufficient vacuum region to describe noninteracting polymer chains in the perpendicular directions. A London correction[25] to dispersive forces is included to improve the description of distortion due to steric hindrance. Each structure is fully relaxed, until forces on all atoms become lower than 0.03 eV/Å. Vibrational properties are evaluated from first-principles by means of a Density Functional Perturbation Theory[26] approach, also implemented in Quantum-ESPRESSO package.

Optical Properties. The UV–vis spectra are computed for a set of oligomers with increasing length: convergence was reached with eight monomer units for PFO, and six monomer units for PFP and PFTFP. We adopted the framework of the semiempirical Hartree–Fock (HF) based method ZINDO[27] through the configuration interaction (CI) procedure, including single excitations only (ZINDO/CIS). This method is known to provide reliable results for aromatic systems.[28] All calculations are performed starting from optimized geometries

dx.doi.org/10.1021/jp409996m | J. Phys. Chem. C 2013, 117, 26760–26767

(0.4 kcal·mol^{-1}/Å force threshold) and mean-field ground-state properties are calculated with AM1.[29,30]

3. RESULTS AND DISCUSSION

3.1. Characterization of PFTFP Polymer. The PFTFP copolymer was synthesized via Suzuki cross-coupling, one of the best synthetic protocols for industrial production of optoelectronic materials, as reported in ref 23. PFTFP results from the insertion of a fluorinated phenyl ring along the PFO main axis, as shown in Scheme 1. The perfluorination does not affect the solubility of the copolymer in common organic solvents, while it influences thermal and mechanical properties of the material. In fact, no glass transition was observed in the range of 50−200 °C.[23] This behavior differs from the standard PFO, where phase transitions are observed around 80 and 150 °C,[31] due to the organization of the alkyl chains and melting. This observation, together with the small difference observed between the absorption and emission spectra in solution and in solid state (around 5 nm) and the exceptionally high PLQY (≈68%) retained in the solid state film, suggests that (i) despite the presence of lateral alkyl chains, PFTFP neither interdigitates nor forms agglomerates; (ii) the polymeric conformation is quite similar in solution and solid state, suggesting a polymeric isolation also in the solid state. On the basis of these conclusions, here we assume the single polymer as representative of the main properties of the PFTFP material.

We use atomistic first principles calculations to reproduce and interpret the experimental results. The theoretical atomic structure is reported in Figure 1a, where we substituted the two C_8H_{17} alkyl chains with methyl groups. The theoretical pitch of the periodic chain (13.02 Å) has been obtained by minimizing the total energy of the system, as a function of the cell dimension in the direction along the polymer. After total-energy-and-forces optimization, average F−C distance is 1.37 Å, the inter-ring distance C2−C3 (see labels in Figure 1a) is 1.51 Å and the fluorinated phenylene is rotated by only 44.3° (torsion angle C1−C2−C3−C4) with respect to the PFO plane. One long-debated question in the literature is whether or how much such angular rotation is due to the presence of the F substituent. In the present case, the inclusion of fluorinated phenyl ring mostly preserves the planarity of the pristine PFO system. We return later on this point.

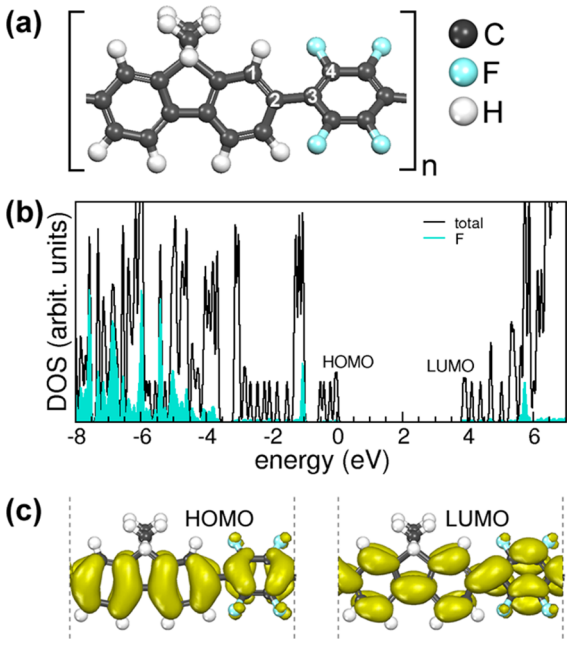

Figure 1. (a) Ball-stick representation of PFTFP monomer used in the simulation of periodic polymers. Chemical elements are explicitly reported on the right. White labels indicate specific C atoms discussed in the text. (b) Calculated total and F-projected density of states of periodic PFTFP system. Energy reference zero is aligned to HOMO. (c) Isosurface charge density plots of single-particle frontier orbitals.

As a crosscheck test on the structure and composition of PFTFP, we compared the experimental and theoretical infrared (IR) spectra, as shown in Figure 2. Fourier Transform Infra

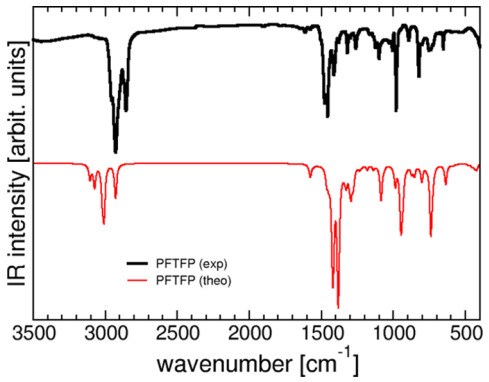

Figure 2. Experimental (black line) and theoretical (red line) IR spectra of PFTFP.

Red (FTIR) spectrum of PFTFP (black line) is dominated by two main vibrational branches: the first one (2855−3100 cm^{-1}) corresponds to the high frequency C−H stretching modes of the PFO subunit; the second one (700−1500 cm^{-1}) shows several peaks that can be attributed to ring stretching and breathing modes. Alkyl C−H rocking modes are at ∼820 cm^{-1}. The strong double peak around 1400 cm^{-1} is attributed to the presence of CF bonds in the phenyl ring. A part a small blue-shift of the higher frequency branch of ∼70 cm^{-1}, the theoretical spectrum (red line) well reproduces all the features of the experimental one. The slight discrepancy of the optical C−H stretching branch is partially due to the substitution of the entire C_8H_{17} alkyl chains with the methyl groups. Nonetheless, this confirms the validity of the model we used for simulations.

The calculated electronic structure is summarized in Figure 1b, where the total and F-projected density of states (DOS) is displayed (numerical data are also reported in Table 1 along with experimental results). The polymer has a semiconducting behavior with a calculated DFT HOMO−LUMO gap E_g = 3.9 eV. This is in very good agreement with the experimental values of the cyclic voltammetry (CV) measurements (E_g = 3.8 eV). In a similar way, the calculated HOMO/LUMO levels (−6.3/−2.4 eV), which are directly related to the ionization potential and electron affinity of the system, perfectly match the electrochemical ones (−6.2/−2.4 eV), confirming the validity of the adopted 1D model in catching the main properties of the system. The highest occupied and lowest unoccupied peaks in the DOS have a finite width (∼0.6 eV) that corresponds to the establishment of dispersive energy bands along the polymer direction.[32] The effective masses for electron (m_e*) and holes (m_h*), evaluated as the inverse of the second derivative of the energy bands versus the crystalline momentum **k** in the

dx.doi.org/10.1021/jp409996m | J. Phys. Chem. C 2013, 117, 26760−26767

Table 1. Effective Electron (Hole) Masses m_e^* (m_h^*) Energy Gaps, HOMO and LUMO Energy Levels for PFTFP, PFO, and PFP Polymers, from Theoretical Calculation, Electrochemistry Measurements, and Absorption Spectra[a]

	theory						electrochemistry			absorption spectra
	m_h^*	m_e^*	HOMO	LUMO	E_g (DFT)	E_{opt} (CI)	HOMO	LUMO	E_g	E_{opt}
PFO	0.150	0.148	−5.4	−2.0	3.4	3.5	−5.6	−2.2	3.4	3.2
PFP	0.241	0.219	−5.8	−1.9	3.9	3.6	−5.8	−2.2	3.6	3.4
PFTFP	0.241	0.211	−6.3	−2.4	3.9	3.7	−6.2	−2.4	3.8	3.6

[a]All energy values are given in eV, effective masses in unit of the free electron. We distinguish the electrical gap, E_g, related to the HOMO−LUMO gap, and the optical gap, E_{opt}.

parabolic approximation, are 0.21 and 0.24, respectively, and are representative of a high intrinsic intrachain conductivity of the polymer. Indeed, these remarkable band widths (or alternatively low effective masses) are the fingerprint of the establishment of delocalized (Bloch-like) electronic states along the chain, available for intrachain charge transport even in the presence of F atoms. This is confirmed also by the character of the HOMO and LUMO states (Figure 1c), which are purely π-like conjugated states distributed across the entire PFTFP units; that is, we do not observe any specific charge localization due to fluorine either in the PFO or in phenylene subunit. The projection of F-contribution in the DOS (Figure 1b) confirms that F-derived states become relevant more than 1 eV below (above) the HOMO (LUMO). This result is in contrast, for instance, with the work by Chang and co-workers[33] on indacenodithieno[3,2-*b*]thiophene arene units, where the LUMO is strongly localized on the acceptor moiety of the polymer monomeric units. However, calculations of Chang's work regarded only the monomeric units.[32] Here instead DFT calculations are extended to along the whole polymeric chain: the conjugation is favored by the "polymeric effect" and a delocalization of the LUMO level along the polymer backbone is not surprising.

We can thus conclude that PFTFP polymer is an ordered system, with a well-defined semiconducting behavior, deriving from the extended π-conjugation of frontiers orbital across the entire polymer, which assures good intrinsic intrachain conduction properties to the material. Evidently, the final conductivity of the polymeric system measured in a solid state device will be affected also by other interactions such as disorder, defects, interchain hopping, polaronic effects, and contact barrier that reduce the effective transport efficiency of the system. We note also that the electron/hole effective masses resulting from ab initio calculations are very similar, despite the fact that experimentally the hole mobility in conjugated polymers is in general several orders of magnitude larger than the electron mobility.[34] This discrepancy has been already discussed in the literature[35] and the higher hole mobility has been ascribed to several effects: (i) compensation of the hole traps by p-doping; (ii) electron traps caused by oxidation; (iii) structural defect level in solid state films. Indeed, microwave experiments demonstrated that the electron and hole mobilities are similar when the polymer chains are isolated in solution.[36]

3.2. Effect of Fluorination. As mentioned above, the nature and origin of the fluorination effects are still not clear.[37] For some authors it is mainly a geometrically driven effect,[13] while for others the purely electronic mechanism is prevalent and must be separated from the geometric one.[38] In order to gain insights into the effects of the fluorination on the structural and electronic properties of the polymer, we performed a systematic experimental/theoretical comparison with plain PFO and hydrogenated PFP chains (see Scheme 1). The former is assumed as the reference system for this class of materials, and the latter makes evident the effect of F decoration.

On the structural point of view, the theoretical results show that the minimum energy geometry of PFP polymer is almost identical to the PFTFP one. Indeed, the inclusion of H instead of F does not change either the periodicity of the polymer or the inter-ring distance C2−C3 (now 1.52 Å). The phenyl ring results to be rotated by 42.7° with respect to the PFO plane, less than 2° of difference with the fluorinated counterpart. This means that the loss of the perfect planarity is not due to F itself but to the inclusion of the phenylene subunits and to the steric effects between its decorating species (both H and F) and the closest hydrogen atoms of the PFO unit. The similar van der Waals radii of fluorine (1.35 Å) and hydrogen (1.20 Å) justify the similar final rotated geometries of the two systems.

Such torsion angle still preserves the π-conjugation along the polymer, contrary to other systems where F is directly attached to the vinyl group and the resulting strong geometric distortion is detrimental to the electron (band-like) properties of the polymer.[13] In this case, the loss of ideal planarity, with respect to PFO, only slightly reduces the dispersion of the bands close to the Fermi level, the ones involved in carrier transport processes (see the band-structure comparison reported in Figure S1 of the Supporting Information, SI). This reduction may be quantified in terms of the calculated effective masses, reported in Table 1. The presence of the phenyl units makes the electron and hole effective masses heavier (i.e., reduction of carrier mobility), but still similar to other conjugated polymers (e.g., PEDOT/PSS) or wide-band gap semiconductor materials (e.g., GaN, ZnO) routinely used in electronic devices. The inclusion of F is thus irrelevant for this aspect: significant values for the effective masses are maintained. This means that the residual torsion angle in the PFTFP does not waste the charge transport and the polymer efficiently behaves as a good semiconductor. In order to confirm this statement, we consider a further configuration (see Figure S3 in SI), where we substituted the perfluorinated ring of PFTFP with a *trans*-2−5-trifluoromethyl-benzene. In this case, the larger spatial hindrance of the CF_3 lateral group increases the torque angle (52.2°) with respect to the PFO plane. As a consequence this reduces the conjugation (i.e., band dispersion) of the polymer, but it does not foster any further F contribution to the frontier orbitals (see section S2 in SI), even though the monomer includes 50% fluorine atoms more than PFTFP. It turns out that the effects of F on the structure of conjugated polymers is not ubiquitous but rather is strictly dependent on its position with respect to the C-conjugated chain.

An important point to clarify is the interplay between the conjugation of the C-based polymer and the electrostatic interaction due to the charge accumulation intrinsically localized around F atoms. Indeed, the fact that we do not

dx.doi.org/10.1021/jp409996m | J. Phys. Chem. C 2013, 117, 26760−26767

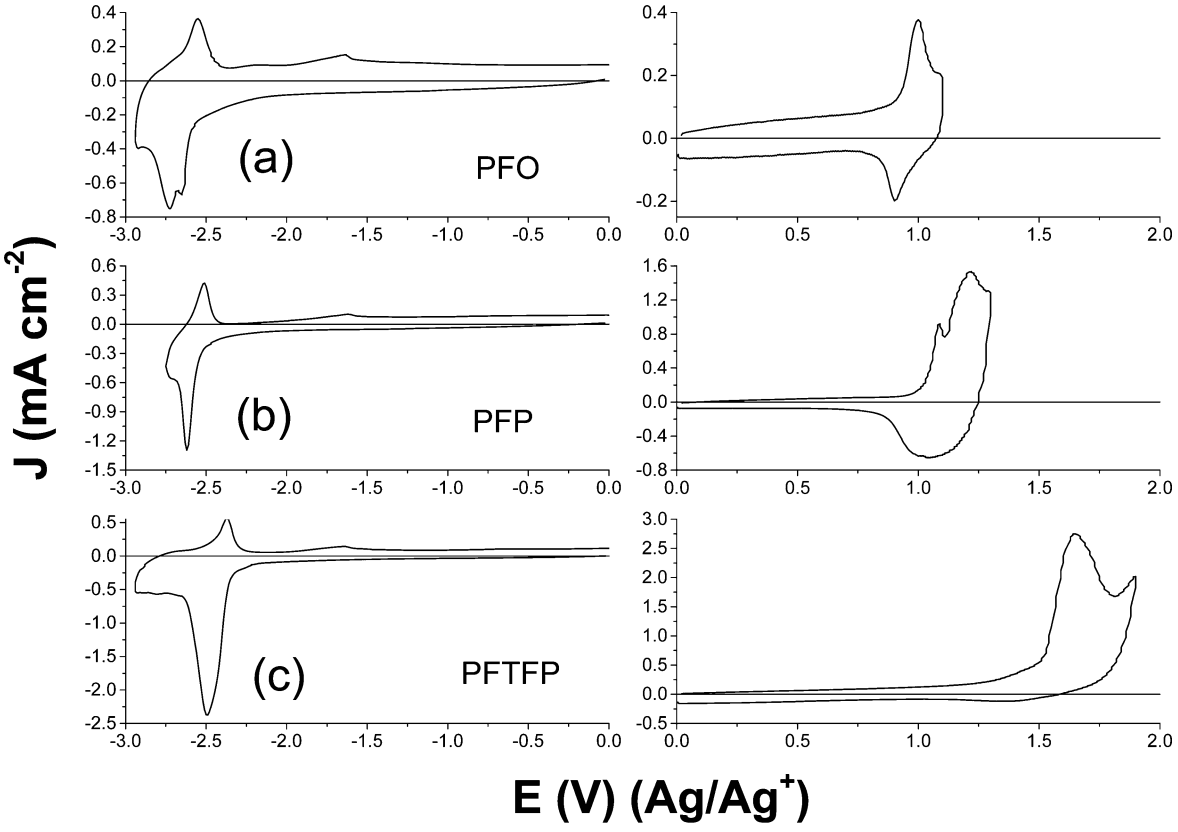

Figure 3. Oxidation (right side) and reduction (left side) cyclic voltamograms of (a) PFO, (b) PFP, and (c) PFTFP. CVs measurements are performed in AN+TBAP 0.1 M as cast film[35] on glassy carbon electrode of 0.2 cm^{-2} of area, Ag/Ag^+ as reference electrode.

observe any direct contribution of F on the charge distribution (conjugation) of the frontiers orbitals does not imply that fluorine does not have any effect of the overall electronic properties of the chain. To demonstrate this, cyclic voltammetry (CV) measurements were conducted on drop-cast polymer films[39] on carbon-glass working electrode (0.2 cm^{-2}). Figure 3 displays the oxidation (right side) and the reduction (left side) CVs of PFO (Figure 3a), PFP (Figure 3b), and PFTFP (Figure 3c). Fluorination markedly influences the oxidation potentials: as reported in Table 2, the PFTFP oxidation potential is 0.44 and 0.7 V, higher than the ones of PFP and PFO, respectively. Remarkably, its effect is less marked on the reduction potentials. PFTFP reduction potential is only 0.15 and 0.2 V lower than PFP and PFO, respectively. From the on-set ionization potentials in the CV measurements we have also evaluated the HOMO−LUMO energy levels (Table 1).

Table 2. Absorption Maxima (λ_{max}) in Toluene Solution and Oxidation and Reduction Peak Potentials (E_{ox}, E_{red})[a] of All Polymers

	λ_{max} (nm)	E_{ox} (V)	E_{red} (V)
PFO	387	0.95	−2.6
PFP	365	1.21	−2.55
PFTFP	345	1.65	−2.4

[a]Ref Ag/Ag^+.

The electrochemical data for PFTFP show a high oxidation potential (see Table 1) and a marked HOMO lowering (Table 1), which is a direct consequence of the electron-withdrawing effect of the fluorine atoms, in agreement with similar experimental results.[33,40] Such aspect suggests a larger resistance against oxidation-related degradation[3] as well as a modification of charge injection into external leads: this is summarized in Figure 4, where the measured HOMO/LUMO energy levels of the polymers are reported in comparison with the oxidation potential of ITO, polyethylenedioxithiophene (PEDOT), and the Fermi level of aluminum.

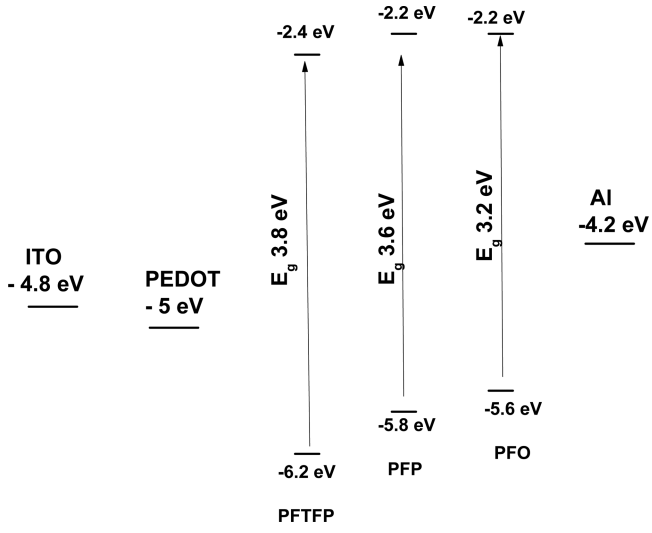

Figure 4. HOMO and LUMO energy levels of PFO, PFP, and PFTFP, together with ITO, PEDOT, and Al energy levels, which are reported for comparison.

The electrochemical data for PFTFP show a high oxidation potential (see Table 1) and a marked HOMO lowering (Table 1), which is a direct consequence of the electron-withdrawing effect of the fluorine atoms, in agreement with similar

dx.doi.org/10.1021/jp409996m | J. Phys. Chem. C 2013, 117, 26760−26767

The fluorinated PFTFP presents the lowest LUMO level and the deepest HOMO level: Going from PFO to PFP, the inclusion of the phenyl ring leaves the energy position of LUMO unchanged, while it slightly lowers by 0.2 eV the HOMO. Inclusion of fluorine affects both HOMO and LUMO that are further shifted by 0.4 and 0.2 eV, respectively, toward lower energies. DFT results quantitatively confirm these findings (Table 1). This indicates that the effect of fluorine is mainly electrostatic: the local charge accumulation around the phenyl ring (that does not affect the frontier orbitals but takes place at lower energies, see DOS) acts as an *effective gate potential* that shifts to different extent both valence and conduction bands, without perturbing the delocalization of the conjugated electrons along the C structure. To confirm this behavior, we performed calculations also on PFTFP monomers, for both flat (not relaxed, not stable) and tilted (energetically favored) configuration (see Figure S4, SI, for details): the results revealed almost no difference between the calculated ionization potentials (i.e., HOMO energy levels) of the two molecule configurations, that is, 6.3 eV for the flat and 6.4 eV for the tilted. DFT calculations on the infinite polymer with a phenylene bearing bulky CF3 described above does not show relevant changes in the ionization potentials (6.4 eV of the CF3 substituted and 6.3 eV of the four fluorine one), confirming the electron-acceptor nature of fluorination, beyond the specific type of fluorine substituent.

We can conclude that lowering of the ionization potential (and thus the higher stability against oxidation) is a quite general effect due to the electron-withdrawing tendency of fluorine. The structural distortion and the consecutive electron localization are instead dependent on the substitution site and on the persistence of the electron conjugation along the polymer. The coexistence of both high electron conjugation and high oxidation stability makes PFTFP an exceptional material, as already shown in a previous report.[23]

3.3. Optical Properties. The HOMO−LUMO gap modifications observed in electrochemical measurements and confirmed by DFT calculation suggest modifications also in the optical properties of the system. Figure 5 reports UV−vis absorption spectra of the three polymers under investigation. The corresponding optical gaps (E_{opt}) are summarized in Table 1. Optical gap differs from electrical one for excitonic effects that tend to reduce the gap. Compared with plain PFO (black-line) and PFP (red line), the main absorption peak of PFTFP (blue line) is blue-shifted by 0.4 and 0.2 eV, respectively. This confirms that fluorination favors the shift of the optical activity of the material in the deep-blue range of the spectrum.

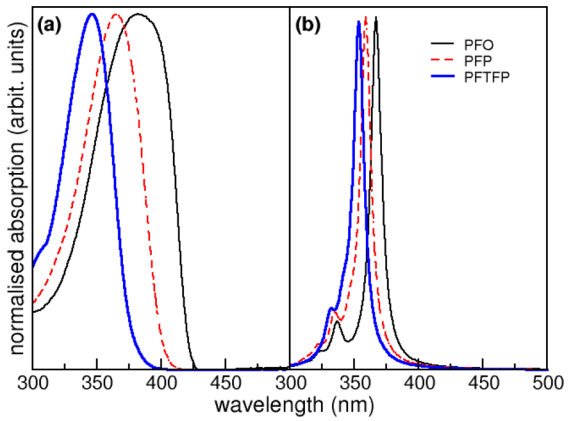

Figure 5. Experimental (a) and theoretical (b) UV−vis spectra of PFO (thin black), PFP (dashed red), and PFTFP (thick blue). Experimental spectra are taken in toluene solution.

The theoretical absorption spectra were obtained by employing standard quantum-chemistry tools, such as the CI scheme on top of semiempirical Hartree−Fock based calculations, and are shown in Figure 5b. Table 1 shows that the calculated optical gaps are quite consistent with the ones obtained from the optical measurements: the blue-shift trend experimentally observed passing from PFO to PFP and PFTFP is well reproduced by the calculations. The absolute values of the optical gaps energy are systematically overestimated by 0.1−0.3 eV with respect to experiments, which is quantitatively consistent with the absence of solvent effects in the calculations. Our theoretical analysis also allows us to associate the lowest-energy peak of the optical spectrum with an excitonic state mainly derived from the optically allowed HOMO−LUMO transition; no low-energy dark states are detected. This is a fundamental result: the presence of dark states in the gap could trap the excitons, giving rise to subgap energy nonradiative phenomena. On the contrary, their absence allows for efficient light emission. This finding agrees with the excellent luminescence efficiency observed for PFTFP,[23] opening the way for their application as deep-blue emitters. In this framework, our properly optimized fluorinated material shows an undisputed advantage with respect to the parent PFO polymers with a PLQY of 68% in solid state higher than the one of PFOP (60%) and of PFO (53%)

We finally note that the 0.2 eV blue-shift of PFTFP absorption edge with respect to PFP is four times lower than the blue-shift reported in ref.[13] for fluorinated MEH-PPVF having F instead of H in the double bound. In that case, the authors ascribed the large blue-shift only to the steric-effect caused by the repulsion between the fluorine atoms and the neighboring alkoxy substituents. Our results show a more complex scenario: PFTFP has a more rigid structure without any alkoxy substituent able to free-rotate and give rise to so high distortions. This almost preserves (as demonstrated above) the pristine electron conjugation along the chain that more efficiently screens the electrostatic effect of the F atoms, reducing the blue-shift of the energy levels.

4. CONCLUDING REMARKS

We presented a detailed experimental and theoretical characterization of a fluorinated polyfluorene derivative (PFTFP) recently synthesized. The direct comparison with PFO and auxiliary derivative systems confirms that fluorination in PFTFP is mostly electronic in nature and affects its electrochemical behavior. In particular, we highlighted three fundamental properties of PFTFP material: (i) The torsion angle between the PFO unit and the phenylene one does not waste the π-like electronic distribution of frontier orbitals along the chain, typical of the conjugated C-based systems. This corresponds to good intrachain electron transport characteristics. (ii) The inclusion of fluorine imparts a low-energy shift of the HOMO and LUMO levels with respect to PFO, which corresponds to an enhancement of the ionization potential and electron affinity, respectively. The increase of the oxidation potential assures a higher stability of PFTFP against oxidation. (iii) Fluorination modifies the optical properties of the system, whose absorption-edge results blue-shifted.

dx.doi.org/10.1021/jp409996m | J. Phys. Chem. C 2013, 117, 26760−26767

The combination of these three characteristics makes PFTFP a unique organic semiconductor, which conjugates the high mobility properties of PFO and the enhancement of oxidation stability and of deep-blue photoluminescence induced by fluorination.

■ ASSOCIATED CONTENT

Supporting Information

Simulated electronic structure of PFO and PFP periodic polymers (sec S1); characterization of an auxiliary PFO-derivative (sec S2); and comparison between tilted and flat monomers (sec S3). This material is available free of charge via the Internet at http://pubs.acs.org.

■ AUTHOR INFORMATION

Corresponding Author

*Phone: +39-059-2055627. Fax: +39-059-2055651. E-mail: arrigo.calzolari@nano.cnr.it.

Notes

The authors declare no competing financial interest.

■ ACKNOWLEDGMENTS

Dr. Gianni Zotti is kindly acknowledged for the fruitful scientific discussions. This work was supported in part by Regione Lombardia through Project "Tecnologie e materiali per l'utilizzo efficiente dell'energia solare" decreto 3667/2013.

■ REFERENCES

(1) Lee, S. R.; Shin, J.-H.; Baek, J.; Oh, M.; Yoon, T. H.; Jae Kim, J. C. *Appl. Phys. Lett.* **2007**, *90*, 163513.
(2) Tang, M. L.; Bao, Z. *Chem. Mater.* **2011**, *23*, 446−455.
(3) Babudri, F.; Farinola, G. M.; Naso, F.; Ragni, R. *Chem. Commun.* **2007**, 1000−1022.
(4) Anthony, J. E.; Facchetti, A.; Heeney, M.; Mardeer, S. R.; Zhan, X. *Adv. Mater.* **2010**, *22*, 3876−3892.
(5) (a) Heidenhain, S. B.; Sakamoto, Y.; Suzuki, T.; Miura, A.; Fujikawa, H.; Mori, T.; Tokito, S.; Taga, Y. *J. Am. Chem. Soc.* **2000**, *122*, 10240−10241.
(6) (a) Stadlober, B.; Zirkl, M.; Beutl, M.; Leising, G.; Bauer-Gogonea, S.; Bauer, S. *Appl. Phys. Lett.* **2005**, *86*, 242902. (b) Schroeder, B. C.; Huang, Z.; Ashraf, R. S.; Smith, J.; D'Angelo, P.; Watkins, S. E.; Anthopoulos, T. D.; Durrant, J. R.; McCulloch, I. *Adv. Funct. Mater.* **2012**, *22*, 1663−1670. (c) Facchetti, A.; Yoon, M. H.; Stern, C. L.; Katz, H. E.; Marks, T. J. *Angew. Chem., Int. Ed.* **2003**, *42*, 3900−3903.
(7) (a) Liang, Y.; Feng, D.; Wu, Y.; Tsai, S.-T.; Li, G.; Ray, C.; Yu, L. *J. Am. Chem. Soc.* **2009**, *131*, 7792−7799. (b) Zhou, H.; Yang, L.; Stuart, A. C.; Price, S. C.; Liu, S.; You, W. *Angew. Chem.* **2011**, *123*, 3051−3054. (c) Wei, Q.; Nishizawa, T.; Tajima, K.; Hashimoto, K. *Adv. Mater.* **2008**, *20*, 2211−2216.
(8) Pasini, M.; Giovanella, U.; Betti, P.; Bolognesi, A.; Botta, C.; Destri, S.; Porzio, W.; Vercelli, B.; Zotti, G. *ChemPhysChem* **2009**, *10*, 2143−2149.
(9) Sakamoto, Y.; Suzuki, T.; Kobayashi, M.; Gao, Y.; Fukai, Y.; Inoue, Y.; Sato, F.; Tokito, S. *J. Am. Chem. Soc.* **2004**, *126*, 8138−8140.
(10) Yamaguchi, Y. *J. Chem. Phys.* **2005**, *122*, 184702.
(11) Cocchi, C.; Prezzi, D.; Ruini, A.; Caldas, M. J.; Molinari, E. *J. Phys. Chem. C* **2012**, *116*, 17328−17335.
(12) Osuna, R. M.; Ortiz, R. P.; Delgado, M. C. R.; Sakamoto, Y.; Suzuki, T.; Hernández, V.; López Navarrete, J. T. *J. Phys. Chem. B* **2005**, *109*, 20737−20745.
(13) Piacenza, M.; Della Sala, F.; Farinola, G. M.; Martinelli, C.; Gigli, G. *J. Phys. Chem. B* **2008**, *112*, 2996−3004.
(14) Park, J. H.; Jung, E. H.; Jung, J. W.; Jo, W. H. *Adv. Mater.* **2013**, *25*, 2583−2588.
(15) Tumbleston, J. R.; Stuart, A. C.; Gann, E.; You, W.; Ade, H. *Adv. Funct. Mater.* **2013**, DOI: 10.1002/adfm.201300093.
(16) Wakioka, M.; Kitano, Y.; Ozawa, F. *Macromolecules* **2013**, *46*, 370−374.
(17) Mercier, L. G.; Leclerc, M. *Acc. Chem. Res.* **2013**, *46*, 1597−1605.
(18) (a) Feast, W. J.; Cacialli, F.; Koch, A. T. H.; Daik, R.; Lartigau, C.; Friend, R. H.; Beljonne, D.; Bredas, J. L. *J. Mater. Chem.* **2007**, *17*, 907−912. (b) Losurdo, M.; Giangregorio, M. M.; Capezzuto, P.; Cardone, A.; Martinelli, C.; Naso, G. M. F.; Büchel, M.; Bruno, G.; Farinola, G. M.; Babudri, F. *Adv. Mater.* **2009**, *21*, 1115−1120.
(19) (a) Grimsdale, A. C.; Chan, K.; Martin, R. E.; Jokisz, P. G.; Holmes, A. B. *Chem. Rev.* **2009**, *109*, 897−1091. (b) Pogantsch, A.; Wenzl, F. P.; List, E. J. W.; Leising, G.; Grimsdale, A. C.; Müllen, K. *Adv. Mater.* **2002**, *14*, 1061−1064. (c) Xiao, S.; Nguyen, M.; Gong, X.; Cao, Y.; Wu, H.; Moses, D.; Heeger, A. J. *Adv. Funct. Mater.* **2003**, *13*, 25−29.
(20) (a) Scherf, U.; List, E. J. W. *Adv. Mater.* **2002**, *14*, 477−487. (b) List, E. J. W.; Guentner, R.; Freitas, P. S. D.; Sherf, U. *Adv. Mater.* **2002**, *14*, 374−378. (c) Zojer, E.; Pogantsch, A.; Hennebicq, E.; Beljonne, D.; Bredas, J. L.; Scandiucci, P.; Scherf, U.; List, E. J. W. *J. Chem. Phys.* **2002**, *117*, 6794. (d) Lemmer, U.; Heun, S.; Mahrt, R. F.; Scherf, U.; Hopmeier, M.; Sieger, U.; Göbel, E. O.; Müllen, K.; Bässler, H. *Chem. Phys. Lett.* **1995**, *240*, 373−378.
(21) Yang, X. H.; Jaiser, F.; Neher, D.; Lawson, P. V.; Bredas, J. L.; Zojer, E.; Guntner, R.; Scanduicci de Freitas, P.; Forster, M.; Scherf, U. *Adv. Funct. Mater.* **2004**, *14*, 1097−1104.
(22) Yoon, M.-H; Facchetti, A.; Stern, C. E.; Marks, T. J. *J. Am. Chem. Soc.* **2006**, *128*, 5792−5801.
(23) Giovanella, U.; Botta, C.; Galeotti, F.; Vercelli, B.; Battiato, S.; Pasini, M. C. *J. Mater. Chem. C* **2013**, *1*, 5322−5329.
(24) Giannozzi, P.; Baroni, S.; Bonini, N.; Calandra, M.; Car, R.; Cavazzoni, C.; Ceresoli, D.; Chiarotti, G. L.; Cococcioni, M.; Dabo, I.; Dal Corso, A.; de Gironcoli, S.; Fabris, S.; Fratesi, G.; Gebauer, R.; Gerstmann, U.; Gougoussis, C.; Kokalj, A.; Lazzeri, M.; Martin-Samos, L.; Marzari, N.; Mauri, F.; Mazzarello, R.; Paolini, S.; Pasquarello, A.; Paulatto, L.; Sbraccia, C.; Scandolo, S.; Sclauzero, G.; Seitsonen, A. P.; Smogunov, A.; Umari, P.; Wentzcovitch, R. M. *J. Phys.: Condens. Matter* **2009**, *21*, 395502 (see also www.quantum-espresso.org).
(25) (a) Barone, V.; Casarin, M.; Forrer, D.; Pavone, M.; Sambi, M.; Vittadini, A. *J. Comput. Chem.* **2009**, *30*, 934−939. (b) Grimme, S. *J. Comput. Chem.* **2006**, *27*, 1787−1799.
(26) Baroni, S.; De Gironcoli, S.; Dal Corso, A.; Giannozzi, P. *Rev. Mod. Phys.* **2001**, *73*, 515−562.
(27) Ridley, J.; Zerner, M. *Theor. Chem. Acta* **1973**, *32*, 111−134.
(28) (a) Caldas, M. J.; Pettenati, E.; Goldoni, G.; Molinari, E. *Appl. Phys. Lett.* **2001**, *79*, 2505−2507. (b) Wang, Z.; Tomovíc, Z.; Kastler, M.; Pretsch, R.; Negri, F.; Enkelmann, V.; Muellen, K. *J. Am. Chem. Soc.* **2004**, *126*, 7794−7795.
(29) Dewar, M. J. S.; Zoebish, E. G.; Healy, E. F.; Stewart, J. J. P. *J. Am. Chem. Soc.* **1985**, *107*, 3902−3909.
(30) AM1 and ZINDO/S calculations were performed using VAMP package included in Accelrys Materials Studio software, version 5.0 (http://accelrys.com/products/materials-studio). We have chosen CI energy windows that include at least 4 eV below HOMO and 3 eV above LUMO, in order to ensure convergence.
(31) (a) Scherf, U.; List, E. J. W. *Adv. Mater.* **2002**, *14*, 477−487. (b) Chen, S. H.; Wu, Y. H.; Su, C. H.; Jeng, U.; Hsieh, C. C.; Su, A. C.; Chen, S. A. *Macromolecules* **2007**, *40*, 5353−5359.
(32) The formation of dispersive energy bands is a typical solid-state effect that cannot be caught by using molecular-like (isolated monomers) theoretical approaches.
(33) Chang, H.-H.; Tsai, C.-E.; Lai, Y.-Y.; Chiou, D.-Y.; Hsu, S.-L.; Hsu, C.-S.; Cheng, Y.-J. *Macromolecules* **2012**, *45*, 9282−9291.
(34) (a) Bozano, L.; Carter, S.; Scott, J.; Malliraras, G.; Brock, P. *Appl. Phys. Lett.* **1999**, *74*, 1132−1134. (b) Blom, P. W. M.; Vissenberg, M. C. J. M. *Mater. Sci. Eng.* **2000**, *27*, 53−94.
(35) Meng, H.-F.; Chen, Y.-S. *Phys. Rev. B* **2004**, *70*, 115208.

(36) Hoofman, R. J. O. M.; de Haas, M. P.; Siebbeles, L. D.A.; Warman, J. M. *Nature (London)* **1998**, *392*, 54−56.
(37) Medina, B. M.; Beljonne, D.; Egelhaaf, H.-J.; Gierschner, J. *J. Chem. Phys.* **2007**, *126*, 111101.
(38) Salzner, U. *J. Phys. Chem. A* **2010**, *114*, 5397−5405.
(39) (a) Jaeger, C. D.; Bard, A. J. *J. Am. Chem. Soc.* **1979**, *101*, 1690−1969. (b) Jaeger, C. D.; Bard, A. J. *J. Am. Chem. Soc.* **1980**, *102*, 5435−5442.
(40) (a) Lu, W.; Kuwabara, J.; Iijima, T.; Higashimura, H.; Hayashi, H.; Kanbara, T. *Macromolecules* **2012**, *45*, 4128−4133. (b) Lu, W.; Kuwabara, J.; Kanbara, T. *Macromolecules* **2011**, *44*, 1252−1255.